HHS Public Access

Author manuscript

Arterioscler Thromb Vasc Biol. Author manuscript; available in PMC 2023 August 01.

Published in final edited form as:

Arterioscler Thromb Vasc Biol. 2022 August ; 42(8): 1060–1076. doi:10.1161/ATVBAHA.122.317643.

Aging alters the aortic proteome in health and thoracic aortic aneurysm

Daniel J. Tyrrell[1], **Judy Chen**[1,2], **Benjamin Y. Li**[1], **Sherri C. Wood**[1], **Wendy Rosebury-Smith**[3], **Henriette A. Remmer**[4], **Longtan Jiang**[5], **Min Zhang**[6], **Morgan Salmon**[5], **Gorav Ailawadi**[5], **Bo Yang**[5], **Daniel R. Goldstein**[1,2,7]

[1:]Department of Internal Medicine, University of Michigan, USA

[2:]Program on Immunology, University of Michigan, USA

[3:]Unit for Laboratory Animal Management, University of Michigan, USA

[4:]Proteomics & Peptide Synthesis Core, University of Michigan, USA

[5:]Department of Cardiac Surgery, University of Michigan, USA

[6:]Department of Biostatistics, University of Michigan, USA

[7:]Department of Microbiology and Immunology, University of Michigan, USA

Abstract

Background: Aging enhances most chronic diseases but its impact on human aortic tissue in health and in thoracic aortic aneurysms (TAA) remains unclear.

Methods: We employed a human aortic biorepository of healthy specimens (n=17) and those that underwent surgical repair for TAA (n=20). First, we performed proteomics comparing aortas of healthy donors to aneurysmal specimens, in young (i.e., <60 years of age) and old (i.e., ≥ 60 years of age) subjects. Second, we measured proteins, via immunoblotting, involved in mitophagy (i.e., Parkin), and also mitochondrial-induced inflammatory pathways, specifically TLR9, STING, and interferon (IFN)-β.

Results: Proteomics revealed that aging transformed the aorta both quantitatively and qualitatively from health to TAA. Whereas young aortas exhibited an enrichment of immunological processes, older aortas exhibited an enrichment of metabolic processes. Immunoblotting revealed that the expression of Parkin directly correlated to subject age in health, but inversely to subject age in TAA. In TAA, but not in health, phosphorylation of STING and the expression of IFN-β was impacted by aging regardless of whether subjects had bicuspid or tricuspid valves. In subjects with bicuspid valves and TAAs, TLR9 expression positively correlated with subject age. Interestingly, whereas phosphorylation of STING was inversely correlated with subject age, IFN-β positively correlated with subject age.

Corresponding author Daniel J. Tyrrell, PhD, University of Michigan, NCRC B020-201-W25, Ann Arbor, MI 48109-2800, dantyrr@umich.edu.

Disclosures: None

Conclusions: Aging transforms the human aortic proteome from health to TAA, leading to a differential regulation of biological processes. Our results suggest that the development of therapies to mitigate vascular diseases including TAA, may need to be modified depending on subject age.

Graphical Abstract

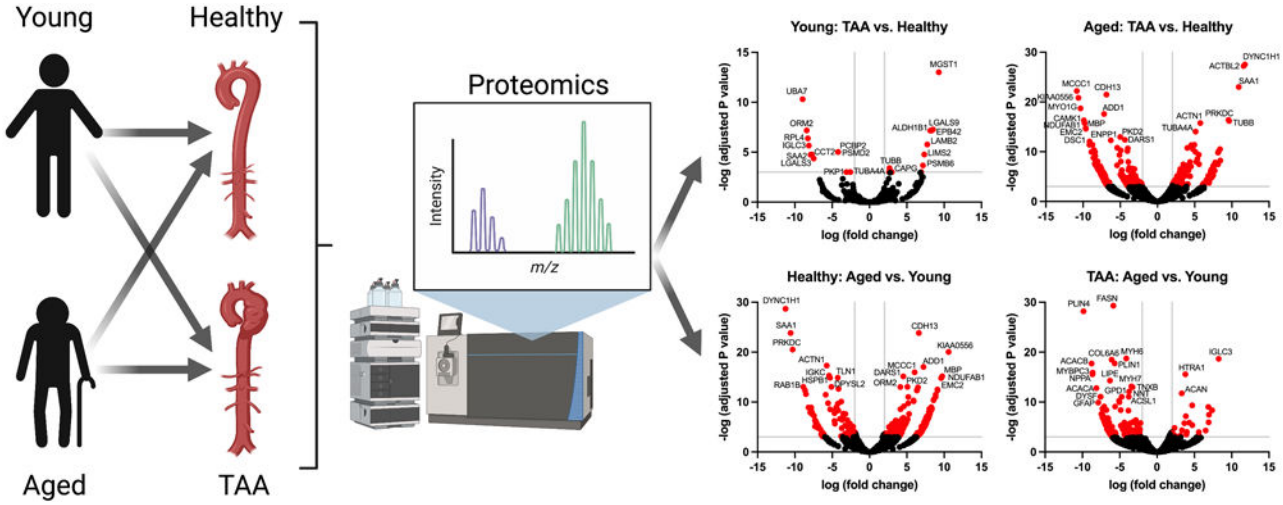

Keywords

Aging; thoracic aortic aneurysm; proteomics

Subject headings:

Translational studies; vascular disease

Introduction

Arterial aging leads to the stiffening of arteries to promote hypertension and accelerate cardiovascular diseases [1]. Several of the classic hallmarks of aging have been implicated in arterial aging and include mitochondrial dysfunction, senescence, and DNA damage [2,3]. Defects in clearing organelles that are damaged by the aging process, via reduced autophagy and mitophagy [4] may also co-exist with these hallmarks and accelerate the aging phenotypes within the vasculature [5,6]. The interplay of the complex effects of aging on the vasculature leads to endothelial cell dysfunction, specifically a reduced ability of these cells to respond dynamically to relaxation and contraction stimuli, and to exhibit a prothrombotic phenotype [7,8]. Vascular smooth muscle cells become more secretory with aging [9], possibly via undergoing senescence, and secrete factors including those that alter the extracellular matrix to stiffen vessels, and inflammatory mediators that promote immune cell recruitment into the vessel during disease, such as atherosclerosis and aneurysm development [8,10]. Most insights into arterial aging come from comparative studies, typically in disease-free rodents [3,9], although there is a recent study in non-human primates [11]. The full scope of changes associated with aging within the arteries in humans remains unclear, and importantly

whether the effects of aging on human arteries differ during health and during disease remains to be elucidated. Given the aging population across the globe, it is imperative to elucidate how human aging impacts the vasculature during health and disease.

Thoracic aortic aneurysm (TAA) is a vascular disease characterized by a 50% increase in aortic diameter [12]. The most characteristic pathology that occurs with TAA is medial layer degeneration, which is characterized by loss of vascular smooth cells, elastic loss of the medial layer, and deposition of proteoglycans [12,13]. The disease is associated with an increase in matrix metalloproteinase-2 and -9 deposition, which promotes degradation of the extracellular matrix. Transforming growth factor (TGF)-β is the main pathologic driver of TAA [12-14]. Genetic syndromes such as Marfan's syndrome are clear risk factors for TAA. Other risk factors include bicuspid aortic valves, inflammatory conditions of the aorta, and hypertension. In non-syndromic TAAs, aging is also a risk factor [15]. However, how aging impacts the aorta in TAA remains unclear.

Here, we used a biorepository of human aortic tissue to examine how aging impacts the aortic proteome between health and disease, specifically TAA. We used 2 different approaches, an unbiased approach via proteomics, and a candidate-based approach, via immunoblotting, based upon prior experimental findings, to investigate the impact of human aging on vascular health and during TAA. Our results show that human aging transforms the aortic proteomic, both quantitatively and qualitatively, between health and disease.

Materials and Methods

The authors declare that all proteomics data are available within the online supplemental files. Because of the sensitive nature of the clinical data collected for this study, requests to access the dataset from qualified researchers trained in human subject confidentiality protocols may be sent to the Institutional Review Board at the University of Michigan.

Biorepository specimens

Human aortic tissues from male and female TAA patients or heart transplant donors from a range of ages were obtained from the Cardiovascular Health Improvement Project core of the Cardiovascular Center at the University of Michigan, with the Institutional Review Board approval from the Human Research Protection Program and Institutional Review Boards of the University of Michigan Medical School. Aortic tissues from patients with TAA were collected during planed surgical procedure for vascular repair with written informed consent. Aortic tissue from healthy control patients were collected at the time of organ recovery for heart transplantation and no informed consent was required. Typically, aortic samples, from the ascending aorta, were free of perivascular fat or calcium and were 2-3mm in thickness and were approximately $1cm^2$ in area. TAA diagnosis was made by the cardiologist and vascular surgeon by imaging. Exclusion criteria was presence of end stage heart failure and abdominal aortic aneurysm. Attrition and randomization were not applicable as the specimens came from a tissue biorepository. Demographics including sex, age, and comorbidities are detailed in Table 1 and for the subset of specimens used in proteomics analysis in Table S1 in the Supplemental Materials. All procedures were

performed in a blinded manner, either using core laboratory services or coded samples in the case of immunoblotting.

Protein immunoblotting

Frozen aortic tissues (~50 mg) were homogenized for 30 seconds in lysis buffer (ThermoFisher Scientific, catalog No. 78510) with 1% protease inhibitor cocktail (Sigma, catalog No. P8340) and 1% phosphatase inhibitor cocktail (Sigma, catalog No. P5726) using a tissue homogenizer (PRO Scientific, Oxford, CT). Tissue lysates were electrophoresed on 4-12% gradient SDS-polyacrylamide gels and transferred to 0.20 μm polyvinylidene difluoride membranes (ThermoFisher Scientific, catalog No. IB40101). Blotted membranes were then blocked in PBS+0.1% Tween-20 +5% BSA for 2 hours at room temperature. Membranes were incubated for 1 hour at room temperature with primary antibodies against Parkin (Abcam, catalog No. ab77924; 1μg/mL), peroxisome proliferator-activated receptor γ coactivator 1-α (PGC1α, Abcam, catalog No. ab54481; 1μg/mL), stimulator of interferon genes (STING; cell Signaling Technology, catalog No. 13647; 0.06μg/mL), phosphorylated-STING (Cell Signaling Technology, catalog No. 19781, 0.05μg/mL), toll-like receptor 9 (TLR9, Santa Cruz Biotechnology, catalog No. sc52966 0.5μg/mL), interferon β (IFNβ, Cell Signaling Technology, catalog No. 73671, 1μg/mL), galectin 9 (LGALS9; Cell Signaling Technology, catalog No. 54330S; 0.1μg/mL), Prohibitin 2 (PHB2, Cell Signaling Technology, catalog No. 14085; 1μg/mL), T-Cadherin (CDH13, Abcam, catalog No. ABT121; 2μg/mL), α−1 acid glycoprotein (ORM2, ThermoFisher Scientific, catalog No. PA5-37124; 1μg/mL), Actin beta-like 2 (ACTBL2, ThermoFisher Scientific, catalog No. PA5-72402; 1μg/mL), and β-Actin (Abcam, catalog No. ab8226; 0.5μg/mL). After washing in PBS+0.1% Tween-20, membranes were incubated in secondary antibodies for 30 minutes at room temperature (Abcam, catalog No. ab205718 and No. ab205719; 0.2μg/mL) and then illuminated with chemiluminescent substrate (ThermoFisher Scientific, catalog No. 34577) using a BioRad ChemiDoc (Hercules, CA). Semiquantitative densitometry was calculated using ImageJ (NIH, Bethesda, MD).

Immunohistochemistry

Formalin-fixed, paraffin embedded aortic tissue blocks were cut at 6μm thick. Slides were deparaffinized using Diva Decloaker (Biocare), blocked (Biocare, catalog No. RBM961) and stained for primary antibodies: Microsomal Glutathione S-Transferase 1 (MGST1; Abcam, catalog No. ab131059, 5.38μg/mL), ACTBL2 (ThermoFisher Scientific, catalog No. PA5-72402, 2μg/mL), CDH13 (Millipore, catalog No. abt121, 0.2μg/mL), LGALS9 (CellSignaling Technologies, catalog No. 55340, 0.27μg/mL), ORM2 (ThermoFisher Scientific, catalog No. PA5-37124, 5μg/mL), and PHB2 (CellSignaling Technology, catalog No. 14085, 1μg/mL). Secondary antibodies were used (Biocare, catalog No. RMR622) followed by 3,3′-Diaminobenzidine (DAB) chromogen and hematoxylin counterstain for nuclei. Slides were scanned and processed using QuPath (version 0.3.2, The University of Edinburgh) and images compiled in GraphPad Prism (version 8.0.0, San Diego, CA).

Proteomic analysis of Aortic tissue

Sample preparation: 25mg of aortic sample were lysed in 100μL of modified radioimmunoprecipitation buffer (2% SDS, 150mM NaCl, 50mM Tris pH8, 1X Roche Complete) and heating at 100°C for 1hr. The protein concentration of the cleared lysates was determined by Qubit fluorometry. 10μg of each sample was processed by SDS-PAGE using a 10% Bis-Tris NuPage Mini-gel with the MES buffer system (Invitrogen). The gel was run 5cm and each gel lane was excised into ten equally sized bands. Gel bands were processed by in-gel digestion with trypsin using a ProGest robot (DigiLab) with the following protocol: (a) Washed with 25mM ammonium bicarbonate followed by acetonitrile; (b) Reduced with 10mM dithiothreitol at 60°C followed by alkylation with 50mM iodoacetamide at RT; (c) Digested with sequencing grade trypsin (Promega) at 37°C for 4h; (d) Quenched with formic acid and analyzed without further processing.

Mass Spectrometry: Half of each digest was analyzed by nano LC-MS/MS with a Waters NanoAcquity HPLC system interfaced to a ThermoFisher Fusion Lumos mass spectrometer. Peptides were loaded on a trapping column and eluted over a 75μm analytical column at 350nL/min using a 0.5hr reverse phase gradient; both columns were packed with Luna C18 resin (Phenomenex). The mass spectrometer was operated in data-dependent mode with the Orbitrap operating at 60,000 FWHM and 15,000 FWHM for MS and MS/MS respectively. The instrument was run with a 3s cycle for MS and MS/MS with Advanced Peak Determination (APD) enabled. A total of 5hrs of instrument time per sample was employed.

Data Processing and Analysis: Data were searched using a local copy of Mascot with the following parameters: Enzyme, Trypsin/P; Database, SwissProt Human (concatenated forward and reverse plus common contaminants); Fixed modifications, Carbamidomethyl (C); Variable modifications, Oxidation (M), Acetyl (N-term), Pyro-Glu (N-term Q), Deamidation (N,Q); Mass values, Monoisotopic Peptide Mass Tolerance of 10 ppm and Fragment Mass Tolerance of 0.02 Da; Maximum Missed Cleavages: 2; Mascot DAT files were parsed into Scaffold (Proteome Software) for validation, filtering and to create a non-redundant list per sample. Data were filtered using 1% protein and peptide FDR and requiring at least two unique peptides per protein. Subsequently the protein lists for each sample together with the total spectrum count were exported to excel. Raw spectral counts were processed in R (version 4.1.0) using edgeR (version 3.34.1) to generate normalized counts using Trimmed Mean of M-values normalization which is a widely used normalization method that produces similar results to Relative Log Expression and Median Ratio Normalization using real and simulated datasets[16,17]. Batch correct was performed by blocking samples by batch. Batch 2 was used as the reference batch due to its larger sample size (batch 2 n =12, batch 1 n=4). The quasi-likelihood genewise dispersions were calculated using the glmQLFit function. Differentially expressed proteins between conditions were calculated by a quasi-likelihood negative binomial generalized log-linear model by using the glmQLFit function. False discovery rate (FDR) q values (adjusted p-values) were used to correct for multiple comparisons. A value of FDR = 0.05 was used as a threshold for statistical significance. Gene ontology (GO) biological processes from up and down-regulated proteins were identified using g:Profiler[18]. All known genes associated with

statistically significant proteins were identified and Benjamini-Hochberg false discovery rate (0.05) was used to generate top significant GO biological processes. Unique GO biological processes were identified and displayed. For example, if the GO terms “Positive regulation of immunity” and “Regulation of immunity” were both identified in the top 10 GO terms, only one of these terms would be presented to reduce redundancy. All statistically significant differentially expressed proteins from each group were also analyzed for network connectivity via STRING analysis[19].

Proteomics Comparisons: Demographic details of the subset of specimens used in the proteomics study can be found in Supplemental Table S1. The proteomics data from 4 groups were compared between: 1) young healthy and young TAA; 2) aged healthy and aged TAA; 3) young healthy and aged healthy; and 4) young TAA and aged TAA.

Statistical Analysis

All results are presented as mean ± standard deviation. For protein immunoblot analysis, subject age was treated as a continuous variable and protein expression level was correlated with age using Pearson correlation coefficients and presented as regressions using GraphPad Prism (version 8.0.0, San Diego, CA). Only male subjects were included in proteomics analysis because we had access to more male subjects than female subjects over a wider range of ages. Due to the broad range of ages included in this study, we did not examine sex as a biological variable; however, future studies should explore this. P values of ≤0.05 were considered statistically significant for these. The authors had full access to all the data in the study and take responsibility for its integrity and the data analysis.

Results

Patient demographics

To investigate how aging impacts arterial aging through health and during disease, we utilized a biorepository containing aortas from individuals with and without vascular disease. The disease-free cohort were donors for organ transplantation and were procured at the time of harvest for organ transplantation, including heart transplantation. The aortas from this cohort were not known to exhibit vascular diseases ante-mortem and were considered healthy. The disease cohort arose from patients with TAA. These samples were harvested during the surgical repair of the aneurysm. In the TAA cohort, none of the subjects had genetic syndromes associated with TAA, although > 75% of patients had bicuspid aortic valve, a condition that associates with TAA [13]. The thoracic aortic aneurysm diameter within the subjects <60 years was 44.2 mm compared to 48.4 mm in those ≥60 years of age; however, there was no significant statistical difference in TAA diameter between the age groups. Demographic and comorbidity characteristics for the 37 individuals in both cohorts are displayed in Table 1 and the demographic characteristics of the subset of samples used in proteomic analysis (see below) are detailed in the Table S1 of the Supplemental Materials.

Aging transforms the aortic proteome from healthy to TAA

We first employed a non-biased approach to investigate how aging impacts the aortic proteome between health and disease, specifically TAA. To do so, we randomly selected

a subset of young (i.e., <60 years of age) and older (i.e., ≥ 60 years of age) male aortic samples from both the healthy subjects and subjects with TAA (i.e., n = 4 biological replicates per age group, all 8 TAA subjects had bicuspid aortic valves) and performed mass spectrometry of the tissue lysates (see methods). We compared healthy aortas to TAA aortas within each age group. Within the young group a total of 22 proteins were statistically significantly altered by TAA. Please note that age was significantly increased in the young TAA vs. young healthy (mean age, young TAA = 46.5 years vs. young healthy group, mean age = 32.75 years, Table S1). Thus, these 22 proteins could be the result of both subject age and TAA. Of these, 11 proteins were significantly upregulated, and 11 proteins were significantly downregulated (Table S2 in the Supplemental Materials). However, in the aged cohort, the number of proteins altered by TAA was much greater at 295 total differentially expressed proteins. Of these, 101 proteins were significantly upregulated and 194 were significantly downregulated (Table S3 in the Supplemental Materials). Volcano plots within each of the young and aged cohorts illustrate how aging transforms the aortic proteome from health to TAA quantitatively (Figure 1A-B). Not only were the number of dysregulated proteins increased within the aged cohort, but there were few shared proteins between the age groups, suggesting there are qualitative changes with aging as well. Histograms for the log fold-change for all identified differentially expressed proteins within the young and aged groups comparing health to TAA demonstrated significantly more proteins with zero fold-change in the young group (Figure 1C) compared to the aged group (Figure 1D) indicating fewer altered proteins in young than aged.

We also performed a STRING analysis (Figure 1E-F) to gain a deeper understanding of the predicted or known interactions between the differentially expressed proteins identified by the proteomics analysis[19]. Due to the lower number of differentially expressed proteins in the young cohort, we found few interactions; however, 3 networks emerged, including galectin-related proteins, molecular chaperone and microtubule proteins, and protein-binding proteins (Figure 1E). In contrast, in the aged cohort, we found 3 networks with more intra- and inter-connections with 3 overall themes with the most interaction between the collagen and integrin-related proteins, followed by proteins related to cytoskeleton and then mitochondria and metabolism (Figure 1F).

Within the proteins that were differentially expressed by TAA in the young and aged groups, we identified only 6 proteins that were dysregulated in both young and aged cohorts, from health to TAA (Table S4 in the Supplemental Materials). These 6 proteins included alpha-1-acid glycoprotein 2 (ORM2), which is a relatively unknown acute phase reactant that has been shown to be elevated in plasma and colon tissue of patients with colorectal cancer, and downregulated in patients with early non-small cell lung cancer [20-22]. The other proteins included Tubulin alpha 4A chain and Tubulin beta chain, which are both cytoskeleton-related proteins that maybe involved in vascular inflammation [23]; and Prohibitin-2 (PHB2) a mitochondrial localized protein involved in stabilizing mitochondria during stress and longevity [24]. PHB2 also has a role in regulating Parkin-mediated mitophagy [25]. Interestingly, the beta-galactosidase, Galectin-3 (LGALS3) was significantly downregulated in both age groups, while another beta-galactosidase, Galectin-9 (LGALS9), a negative regulator on the NLRP3 inflammasome [26], was significantly upregulated in the young group but significantly downregulated in the aged group by TAA. LGALS9 was the only of one of these 6 proteins

we found to be differentially expressed in opposing directions between the age groups and will require future investigation to understand the mechanistic implications.

We next performed a different but complementary analysis to further examine the expression of several proteins identified by the proteomics analysis. Specifically, we examined PHB2, LGALS9, CDH13, ORM2, and ACTBL2 proteins within the aorta with aging. We performed western blots to examine PHB2, LGALS9, and ORM2 because these proteins were significantly altered by TAA in both young and aged groups. We also examined CDH13 and ACTBL2 by western blot as CHD13 was downregulated, and ACTBL2 was upregulated, in TAA vs. healthy within the aged group. We also attempted to examine MGST1 as it is the top upregulated protein in the young TAA group versus young healthy; however, the antibody did not produce a signal in western blots in our hands. We asked within the entire healthy group (n = 17 subjects, both male and female) or the TAA group (n = 20 subjects, both male and female), if aging impacted the expression of these proteins, which we assessed by immunoblotting. We found that expression of PHB2 positively correlated with age in both the healthy ($R=0.551$, $P=0.022$) and TAA groups ($R=0.507$, $P=0.0255$; Figure S1A-B in the Supplemental Materials). Expression of LGALS9 increased with age in aortas from patients with TAA ($R=0.639$, $P=0.0024$) but not in the healthy group (Figure S1 C-D in the Supplemental Materials). We found that both the top band for CDH13 (pro-form), bottom band for CDH13 (mature form), and ACTBL2 were not significantly associated with age in both healthy and TAA groups (Figure S1 E-H and K-L in the Supplemental Materials). Finally, we found that ORM2 significantly positively correlated with age in the healthy group ($R=0.487$, $P=0.048$) but significantly negatively correlated with age in the TAA group ($R=-0.495$, $P=0.0265$; Figure S1 I-J in the Supplemental Materials). In these analyses, we analyzed bicuspid aortic valve (BAV) and tricuspid aortic valve (TAV) samples together; however, we also assessed whether the correlations changed if the BAV samples were analyzed alone. Analyzing the BAV samples alone did not alter whether any of these findings were significant or not. We did not have enough TAV samples to analyze them on their own. Overall, these data indicate, in agreement with the proteomic analysis, that PHB2, LGALS9, and ORM2 are impacted by TAA with their expression altered with aging.

To provide anatomical localization within the aorta of proteins identified by the proteomic analysis, we performed immunohistochemistry for ACTBL2, CDH13, LGALS9, ORM2, PHB2, and MGST1 in paraffin-embedded aortic samples from patients with TAA (Figure S2 in the Supplemental Materials). We selected the same proteins from the western blot analysis with the addition of MGST1, which was upregulated in young TAA vs. young healthy and downregulated in aged TAA vs. young TAA. Immunohistochemical analysis revealed that ACTBL2 and CDH13 localized throughout the aortic cross-section. ORM2 and MGST1 localized to nuclei throughout the aortic cross-section; however, MGST1 also demonstrated staining in the cytosol, particularly near the intimal region. PHB2 demonstrated less staining overall and was localized to nuclei near the intimal region. LGALS9 demonstrated nuclear staining in distinct focal streaks of approximately 300-400μm in length throughout the medial layer. As these data are limited to samples with TAA, represent only 4 biological samples, and only capture a single cross-section of part of the tissue, we have not performed a quantitative assessment of expression levels in these samples. Overall, these data indicate

distinct tissue specific localization within the aortic wall for some of the proteins (ACTBL2, MGST1, and CDH13) while others are distributed throughout the tissue (ACTBL2, CDH13, PHB2, and ORM2). In addition, several proteins are localized to the nuclear compartment (ORM2, MGST1, PHB2, and LGALS9), while others were expressed in the cytosol and extracellular space (ACTBL2, CDH13, and MGST1). Overall, these data show that the proteins identified by our proteomic analysis exhibit varied anatomic expression within the aorta wall in patients with TAA.

Aging alters the biological pathways impacted by TAA

We next performed gene ontology analysis to identify the biological processes that were upregulated and downregulated between health and TAA in the young (Table S5 in the Supplemental Materials) and aged (Table S6 in the Supplemental Materials) cohorts. Overall, the pathway analysis revealed that in the top 10 statistically significantly up- and down-regulated pathways, there was only one shared downregulated pathway: neutrophil mediated immunity, and no shared upregulated pathways when comparing the healthy to the TAA group between the 2 age cohorts (Figure 2 A-D). In the young group, upregulated processes were enriched for immunology processes and included: regulation of mitotic cell phase regulation; immune related processes including NF-κB signaling, leukocyte mediated cytotoxicity, natural killer cell mediated killing and T cell death; cellular response to lipid hydroperoxide; and membrane-based processes including docking and development (Figure 2A). The top 10 most statistically significantly downregulated processes within the young between health and TAA cohort were also enriched for immunological pathways, for example neutrophil mediated immunity, antigen receptor mediated signaling, negative regulation of type I interferon (IFN), and regulation of immune response (Figure 2B). Other less obvious processes that were downregulated within the young cohort between health and TAA included mRNA/RNA catabolic process and cell recognition (Figure 2B).

In contrast to the young cohort, pathway analysis of the aged cohort from health to TAA revealed the following top 10 statistically significantly upregulated processes: blood coagulation, extracellular matrix organization, cell adhesion, and receptor mediated endocytosis and fibrinolysis (Figure 2C). The only immunological process that was in the top 10 significantly upregulated processes in the aged cohort, in comparing health to TAA, related to neutrophil activation and phagocytosis (Figure 2C). The top 10 statistically significantly downregulated processes in the aged cohort from health to TAA enriched for processes related to metabolism. These processes included cellular respiration, ATP production, electron transport chain function, mitochondrial transport, metabolic processes, hexose metabolic response, small molecule catabolic response, and response to oxidative stress (Figure 2D). Overall, within the aged cohort, metabolic processes were impacted by TAA, and processes relating to mitochondrial function were downregulated. In the aged cohort there was a paucity of obvious immunological processes (3 process / total 20 noted) that were impacted from the transition from health to TAA, in sharp contrast to the young cohort in which 9 of the top 20 processes altered by TAA related to immunological processes.

In addition, the GO biological processes that were impacted in the aged cohort (adjusted P values from $4.71x10^{-19}$ to $3.08x10^{-7}$) reached much higher levels of statistical significance compared to the young cohort (adjusted P values from 0.0031 to $1.46x10^{-6}$), owing to the much larger number of differentially expressed proteins in the aged vs. young cohort. These findings largely corroborate what we identified with the STRING analysis above that within the aged cohort, aging impacted metabolic processes between health and TAA. Overall, the pathway and STRING analysis suggest that aging transforms the biology of the TAA disease process within the aorta.

Proteomic analysis of the aorta during health, and TAA

We next re-analyzed our data but examined the impact of aging within the healthy and TAA groups (i.e., comparing healthy subjects <60 years of age to subjects >60 years of age, and similar analysis within the TAA group). Within the healthy group, we found 307 statistically significant differentially expressed proteins (Table S7 in the Supplemental Materials), with 205 upregulated and 102 downregulated when comparing between young and aged subjects, displayed as a volcano plot (Figure 3A). Within the TAA group, we found 19 statistically significantly differentially expressed proteins (Table S8 in the Supplemental Materials), with 10 upregulated and 9 downregulated when comparing young to aged subjects, displayed as a volcano plot (Figure 3B). Histograms of the log fold-change for all identified differentially expressed proteins for the healthy and TAA groups comparing young to aged are displayed in Figures 3 C-D. These results demonstrate that significantly more proteins have a zero fold-change within the TAA group comparison with age as compared to the effect of age within the healthy group. We also performed STRING analysis on the differentially expressed proteins within the healthy cohort between the young and groups, identifying 3 distinct interaction networks. Specifically, within the healthy group comparing the aged to the young cohort, we identified protein interaction networks relating to extracellular matrix, ribosomes and translation, and purine and amino acid metabolism (Figure 3E). Within the TAA group, comparing the aged to young cohort, we identified 3 much small networks relating to microtubules, extracellular matrix, and actin-related proteins (Figure 3F).

To better understand the biologic processes that are impacted by aging in health and in TAA, we analyzed the gene ontology biologic processes (Table S9 and S10 in the Supplemental Materials). Within the healthy group, we found that the top 10 statistically significantly upregulated processes by aging relate to metabolism including small molecule catabolic processes, mitochondrial transport, ATP metabolism, and response to oxidative stress (Figure 4A). The only immunologic process identified in the top 10 statistically significantly upregulated processes was neutrophil immunity. In the healthy aorta the top 10 statistically significantly downregulated processes by aging involved coagulation, extracellular matrix organization, and immunity relating to neutrophil activation and antigen presentation (Figure 4B). Within the TAA group, the number of statistically significantly impacted GO pathways and the overall significance level were reduced compared to the healthy group. The top 10 statistically significantly upregulated processes within the TAA group by aging related to cellular morphology, platelet and thrombin pathways, chaperon mediated protein folding, and immunological processes including the humoral response and natural killer cell differentiation (Figure 4C). The top 10 statistically significantly downregulated processes

within the TAA group by aging related primarily to immunologic processes including response to lipid hydroperoxide, T cell death, regulatory T cell differentiation, dendritic cell regulation, and response to redox state (Figure 4D).

Integrated proteomics analysis reveals overlap between processes in aging and TAA

To integrate all 4 distinct comparisons, we analyzed the differentially expressed proteins from the 4 group comparisons and examined shared differentially expressed proteins in a Venn diagram. This analysis revealed that the groups with the most shared differentially expressed proteins, 197, were found in aged healthy vs. the TAA comparison and healthy young vs. aged comparison (Figure 5A). Furthermore, by using unsupervised clustering (k-means) to analyze the spectral counts from all 16 samples included in the proteomics analysis, we identified 3 differentially expressed clusters that were significantly impacted by both aging and TAA (Figure 5B). An enrichment plot of the significant GO biological processes within the 3 k-means clusters identified the 3 most significant alterations found in these samples to be within immune processes, cytoskeletal remodeling, and metabolism (Figure 5C).

Aging alters aortic Parkin in healthy and in TAA, although in opposing directions

We next performed a candidate-based strategy to examine how aging impacts the aorta within health and then in TAA. This candidate-based strategy was informed by our recent experimental studies in mice and those of others, found that mitophagy is impaired within the vasculature with aging[5,6,27]. We found that impaired mitophagy with aging was associated an upregulation of the mitophagy protein, Parkin within the aorta without evidence of disease [5]. As impaired mitophagy may lead to activation of certain innate immune pathways including Toll like receptor (TLR) and the STING type I IFN pathway[28], we also found that aging within both the aortic and cerebral vasculature led to increased expression of TLR9, STING, and interferon (IFN)-β expression in mice[27]. Given this, we did a targeted analysis of the gene ontology biological processes that were identified within the healthy aorta that were impacted by aging. We searched for the following keywords within the biological processes: parkin, mitophagy, autophagy, senescence, aging, tumor necrosis factor, interleukin, and toll-like receptor. This identified several statistically significant gene ontology biological processes that were impacted by aging including macroautophagy, parkin-mediated mitophagy, aging, regulation of cellular senescence, and regulation of cytokine production (Figure 6A).

We next examined the expression of Parkin, PGC1A, TLR9, STING, and IFN-β within the entire healthy and TAA human cohorts by immunoblotting. We found that aortic levels of Parkin in healthy donor samples positively correlated with subject age ($R=0.627$, $P=0.0071$) (Figure 6B and L). In contrast, in the setting of TAA we found that Parkin inversely correlated with subject age (Parkin: $R=-0.756$, $P<0.0001$, Figure 6C and L). We also examined a regulator of mitochondrial biogenesis, PPAR gamma coactivator 1 alpha (PGC1A) although it did not correlate with subject age in either the healthy or TAA groups (Figure 6 D-E). Overall, these data indicate that aging impacts the expression of a mitophagy protein Parkin within the aorta, but this expression depends on the context: in health, Parkin directly correlates with aging but in TAA Parkin inversely correlates with aging.

Aging impacts the expression of proteins related to inflammation exclusively in the TAA cohort

We examined phosphorylation of STING (p-STING), a signaling protein in the cytosolic DNA sensing pathway, and found that the ratio to STING (i.e., p-STING:STING) inversely correlated with subject age in the TAA group (R=−0.528, P=0.017) but not the healthy group, where no correlation was identified (Figure 6 F, G, and L). Despite p-STING:STING expression negatively correlating with age in the TAA group, IFN-β expression positively correlated with subject age in the TAA group (R=0.446, P=0.049) but not in the healthy group where no correlation between age and IFN-β was identified (Figure 6H, I, and L). In the TAA group, 15 samples had BAV while 5 had TAV. In these analyses, we analyzed BAV and TAV samples together; however, we also assessed whether the correlations changed if the BAV samples were analyzed alone. Analyzing the BAV samples alone did change whether any findings were significant or not except for TLR9 (Figure 6). Specifically, we found that only in subjects that had BAV, TLR9 positively correlated with subject age (R=0.557, P=0.0312) but the significance was lost when examining all BAV+TAV samples together (Figure 6K). TLR activation can lead to production of other cytokines such as IL-6 and TNFα[29], however, we could not detect either of these cytokines via immunoblotting (data not shown). We did not have enough TAV samples to analyze them on their own. Our data show that the expression of p-STING:STING, IFN-β and TLR9 within the aorta did not correlate with aging in the healthy cohort. However, in the TAA cohort, p-STING:STING and IFN-β were impacted by aging. Specifically, p-STING:STING was inversely impacted by aging while IFN-β was directly impacted by aging. This targeted analysis shows that aging impacts the expression p-STING:STING, IFN-β and TLR9 but only in the context of TAA and not in health. Overall, our data suggest that during TAA in subjects with BAV, aging reduces the expression of Parkin along with the expression p-STING:STING and this correlates with activation of the TLR9-IFN-β axis. In health, Parkin is directly correlated with aging but without activation of the TLR9-IFN-β axis.

Discussion

In this study, we found that significantly more proteins are differentially expressed between aged TAA and healthy aged aortic samples as compared to the changes between young TAA and young healthy aortic samples. We also found that comparing healthy aged to healthy young aortas resulted in significantly more differentially expressed proteins compared with the differences observed between TAA aged versus TAA young aortas. Generally, we found that aging enriched for metabolic processes when comparing healthy to TAA (Figure 2), or by comparing aged aortas to young during health (Figure 4). In contrast, young samples generally had an enrichment in immunological processes from health to TAA (Figure 2). Overall, one of the key findings of our study is that aging alters the aortic proteome, both quantitatively and qualitatively, in health and in TAA (Figure 1).

By examining the proteome of young and aged healthy aortas along with young and aged aortas with TAA, we have identified unique proteins impacted by TAA, aging, or both. Galectin 3 (LGALS3) has been implicated in cardiovascular diseases previously and was downregulated by TAA in young samples[30]. Interestingly galectin 9 (LGALS9) was one of

the top upregulated proteins by TAA in the young samples. The top upregulated protein by TAA in young was Microsomal Glutathione S-Transferase 1 (MGST1), which has been implicated in repressing ferroptosis, a form of iron-overload induced cell death program. Thus, the high level of MGST1 may be in response to a high level of ferroptosis in TAA in the young samples[31]. In the aged samples, Dynein Cytoplasmic 1 Heavy Chain 1 (DYNC1H1) and ACTBL2 were the top upregulated proteins. DYNC1H1 is a key subunit of dynein, a crucial cytoskeletal motor protein that converts ATP into mechanical force in muscle cells while ACTBL2 appears to be related to cellular remodeling[32,33]. Future work should uncover how these proteins contribute to the dynamic process of TAA at various ages. Within the healthy aortas, DYNC1H1 was the most significantly downregulated protein while CDH13 was the top upregulated protein by aging. CDH13 was also downregulated in aged TAA samples as compared to aged healthy samples, and it has been implicated in cardiovascular diseases including arrhythmias and heart failure but has not yet been associated TAA[34,35]. In the TAA group, several of the top downregulated proteins with aging are related to cytoskeletal components including myosin heavy chain 6 (MYH6), MYH7, collagen type VI Alpha 6 Chain, and Myosin-binding protein C, while the top upregulated protein was immunoglobulin lambda constant 3 (IGLC3). IGLC3 has been implicated in myocarditis, however, its expression was limited to a subpopulation of B Cells[36]. Our complementary experiments using western blots reveal that some of the proteins identified by our proteomic approach, PHB2, LGALS9, and ORM2 correlated with subject age, while some other proteins, ACTBL2 or CDH13, did not. Possible explanations for these results include that proteomics and western blotting are different techniques with different sensitivities, and we performed the western blotting on a larger sample size with different statistical approaches than the proteomic approach. A limitation of our study is that we do not know what mechanistic role that any of these proteins play in TAA pathogenesis, thus future mechanistic studies will be required to determine the impact of these proteins in TAA pathogenesis and whether they are modified by aging. Nevertheless, our human study provides a rationale for examining these proteins in the future.

We identified that processes related to neutrophil biology were both upregulated (immunity) and downregulated (activation) when we compared healthy aortic samples to TAA samples in the aged group (Figure 2). It is unclear what the implications of these alterations are, and future investigation is needed to understand how aging impacts neutrophil function in healthy vascular aging and during TAA pathogenesis. Another immunological process that we identified in the healthy aorta with aging was downregulation of antigen processing and presentation (Figure 4B). Vascular cells such as endothelial cells can process and present antigens to circulating immune cells, including memory and regulatory T cells [37], which may aid in host defense or promote allo- or auto-immunity [37]. The significance of why aging may reduce antigen presentation within the healthy aorta remains unclear but may be due to age-specific changes in antigen-presenting cells. A reduction in antigen presentation may have implications for adaptive immune responses in the aging aorta. Although we found novel insights in our proteomic analysis of the healthy aorta with aging, some of the identified processes that we found impacted by aging are generally consistent with the current paradigm of vascular aging. In particular, the downregulation of extracellular

matrix pathways and upregulation of metabolic processes with aging may imply alterations in mitochondrial function, which declines with vascular aging [3].

Recent studies have shown the value of proteomics and single cell analysis to identify cellular mechanisms and interactions in vascular diseases including TAA [38-40]. Such analyses have yielded information concerning complex enrichment of cellular clusters, cell-to-cell interactions, and cell trajectories in vascular diseases [38]. Importantly, a recent study has examined the vasculature of healthy young (i.e., 4-6 years of age) and aged (i.e., 18-21 years of age) cynomolgus monkeys, using single cell sequencing [11]. This study identified that the transcription factor *FOXO3A*, a stress responsive factor involved in longevity [41], was downregulated in endothelial cells with aging [11]. Additionally, a prior proteomics study in humans found several highly differentially expressed proteins within aortic media layer with aging, [40]. Although the top protein identified in that study, Lactadherin, was not significantly upregulated in our study, several other top proteins from that study were found in our study, including Lumican, Glutathione S-Transferase Pi 1, Osteoglycin, Thrombospondin 1, Fibronectin 1, and Fibrinogen Alpha Chain [40]. Clearly future studies are warranted to identify which cell types are affected by the biological processes impacted by aging both in health and in TAA that our study has identified.

Our candidate-based strategy here using proteomics and western blotting found a positive correlation with Parkin and age in healthy aortas, which agrees with our previous studies in aged mice that show aging leads to vascular mitophagy dysfunction[5,27]. Interestingly, the correlation of Parkin expression with age was context dependent. In TAA, the correlation was inverse. Changes in Parkin typically reflect an alteration in mitophagy, a dynamic process to remove dysfunctional mitochondria [4]. In our murine models, the increased Parkin expression associated with an impaired mitophagy capacity, specifically to upregulate mitophagy during stress [27]. A reduction in Parkin with aging in the context of TAA could indicate reduced mitophagy, which might be the result of increased destruction of the mitophagic machinery in the aorta with aging during TAA. An alternative non-mutually exclusive explanation is that during aging and TAA there are reduced numbers of total mitochondria, resulting in a reduced activation of mitophagy. Mutations in a protein similar to Parkin, Parkin-like E3 ubiquitin ligase ariadne-1 (ARIH1), are linked to TAA in humans [42]. ARIH1 deletion or mutation was shown to disrupt nuclear and mitochondrial morphology in drosophila, which was rescued by overexpression of Parkin or ARIH1 [42]. Another recent study demonstrated that Parkin expression is reduced in abdominal aortic aneurysms, potentially mediated by production of Factor Xa from platelets [43]. Clarification of the role of Parkin and mitophagy in thoracic and abdominal aortic aneurysms will require future investigation.

We also found, with immunoblotting, that with TAA aging altered the expression of the p-STING:STING ratio, and age positively correlated with aortic expression of IFN-β. The cGAS-STING pathway was originally discovered for sensing DNA in the context of viral immunity and host defense, although it can activate a cell death pathway [44,45]. Phosphorylation of STING typically reflects activation of the pathway [45]. Our measurements reflect a single point in time, and it is possible that during chronic activation of the STING pathway, which occurs during TAA pathogenesis [39], the ratio of p-STING:STING is altered

dynamically. We acknowledge that our study is limited by the fact that all aortic samples were one point in time, although obtaining samples from the same subjects at >1 time point is clearly not feasible in humans. Furthermore, the expression of p-STING:STING could be modulated at the whole tissue level by the degree of cellular apoptosis, which increases in TAA [46,47]. The increase in the IFN-β axis with aging during TAA that we have identified may reflect increased activation of this pathway by mitochondrial components. Another inflammatory mediator, TLR9, was only significantly correlated in the subset of patients with BAV, which suggests there may be a relationship between TLR9 and BAV with vascular aging. BAV increases aortic wall stress[48], which over time could lead to activation of TLR9, an area that will future investigation for verification. With increased mitochondrial dysfunction, mitochondrial DNA may be released and subsequently activate innate immune pathways including the TLR9, inflammasome, and STING pathways [49]. The interaction and interplay of these pathways within the aorta with aging during aneurysm development in general will require future investigation.

In conclusion, our study indicates that aging both quantitatively and qualitatively transforms the biological processes within the aorta from health to the disease state of TAA. Our study implies that biological processes that accompany TAA may also be impacted by aging. This suggests that if novel therapeutics are developed to mitigate against the pathogenesis of vascular diseases, including TAA, these therapeutics may need to be modified according to subject age.

Supplementary Material

Refer to Web version on PubMed Central for supplementary material.

Acknowledgements:

We thank all participants and the collection team of the Cardiovascular Health Improvement Project (CHIP) at the University of Michigan. The collection of samples for Michigan Medicine – Cardiovascular Health Improvement Project was supported by the Frankel Cardiovascular Center. We appreciate the Aikens Fund for Aortic Research and McKay research award for supporting this project. We thank MS Bioworks LLC for experimental processing of the aortic tissue samples. We thank the In vivo animal core in the Unit for Laboratory Animal Management at the University of Michigan for assistance with immunohistochemistry. We thank Dana King for assistance with proteomics analysis.

Sources of Funding:

Grant support: This study was supported by NIH awards: 14SDG18730000 (MS), HL126668 (GA), HL155169, AG028082 (to DRG), AG068309 (DJT), T32GM007863 (BYL), and HL158003 (JC).

NONSTANDARD ABBREVIATIONS AND ACRONYMS

TAA	thoracic aortic aneurysm
TGF	transforming growth factor
PGC1-α	peroxisome proliferator-activated receptor γ coactivator 1-α
STING	stimulator of interferon genes
TLR9	toll-like receptor 9

IFN β	interferon β
LGALS9	galectin 9
LGALS3	galectin 3
PHB2	prohibitin 2
CDH13	T-Cadherin
ORM2	α−1 acid glycoprotein
ACTBL2	Actin beta-like 2
MGST1	Microsomal Glutathione S-Transferase 1
FDR	False discovery rate
GO	Gene ontology
BAV	Bicuspid aortic valve
TAV	Tricuspid aortic valve

References:

1. Wirth A, Wang S, Takefuji M, Tang C, Althoff TF, Schweda F, Wettschureck N, Offermanns S. Age-dependent blood pressure elevation is due to increased vascular smooth muscle tone mediated by G-protein signalling. Cardiovascular Research. 2016;109:131–140. doi: 10.1093/cvr/cvv249 [PubMed: 26531127]
2. Donato AJ, Machin DR, Lesniewski LA. Mechanisms of Dysfunction in the Aging Vasculature and Role in Age-Related Disease. Circulation Research. 2018;123:825–848. doi: 10.1161/circresaha.118.312563 [PubMed: 30355078]
3. Ungvari Z, Tarantini S, Donato AJ, Galvan V, Csiszar A. Mechanisms of Vascular Aging. Circulation Research. 2018;123:849–867. doi: doi:10.1161/CIRCRESAHA.118.311378 [PubMed: 30355080]
4. De Gaetano A, Gibellini L, Zanini G, Nasi M, Cossarizza A, Pinti M. Mitophagy and Oxidative Stress: The Role of Aging. Antioxidants. 2021;10:794. doi: 10.3390/antiox10050794 [PubMed: 34067882]
5. Tyrrell DJ, Blin M, Song J, Wood S, Zhang M, Beard DA, Goldstein DR. Age-Associated Mitochondrial Dysfunction Accelerates Atherogenesis. Circulation Research. 2020;126:298–314. doi: doi:10.1161/CIRCRESAHA.119.315644 [PubMed: 31818196]
6. LaRocca TJ, Hearon CM, Henson GD, Seals DR. Mitochondrial quality control and age-associated arterial stiffening. Experimental Gerontology. 2014;58:78–82. doi: 10.1016/j.exger.2014.07.008 [PubMed: 25034910]
7. Donato AJ, Black AD, Jablonski KL, Gano LB, Seals DR. Aging is associated with greater nuclear NFκB, reduced IκBα, and increased expression of proinflammatory cytokines in vascular endothelial cells of healthy humans. Aging Cell. 2008;7:805–812. doi: 10.1111/j.1474-9726.2008.00438.x [PubMed: 18782346]
8. Gano LB, Donato AJ, Pasha HM, Christopher M. Hearon J, Sindler AL, Seals DR. The SIRT1 activator SRT1720 reverses vascular endothelial dysfunction, excessive superoxide production, and inflammation with aging in mice. American Journal of Physiology-Heart and Circulatory Physiology. 2014;307:H1754–H1763. doi: 10.1152/ajpheart.00377.2014 [PubMed: 25326534]

9. Wang M, Jiang L, Monticone RE, Lakatta EG. Proinflammation: the key to arterial aging. Trends in Endocrinology & Metabolism. 2014;25:72–79. doi: 10.1016/j.tem.2013.10.002 [PubMed: 24365513]
10. Jablonski KL, Donato AJ, Fleenor BS, Nowlan MJ, Walker AE, Kaplon RE, Ballak DB, Seals DR. Reduced large elastic artery stiffness with regular aerobic exercise in middle-aged and older adults. Journal of Hypertension. 2015;33:2477–2482. doi: 10.1097/hjh.0000000000000742 [PubMed: 26378681]
11. Zhang W, Zhang S, Yan P, Ren J, Song M, Li J, Lei J, Pan H, Wang S, Ma X, et al. A single-cell transcriptomic landscape of primate arterial aging. Nature Communications. 2020;11. doi: 10.1038/s41467-020-15997-0
12. Goldfinger JZ, Halperin JL, Marin ML, Stewart AS, Eagle KA, Fuster V. Thoracic Aortic Aneurysm and Dissection. Journal of the American College of Cardiology. 2014;64:1725–1739. doi: 10.1016/j.jacc.2014.08.025 [PubMed: 25323262]
13. Pinard A, Jones GT, Milewicz DM. Genetics of Thoracic and Abdominal Aortic Diseases. Circ Res. 2019;124:588–606. doi: 10.1161/circresaha.118.312436 [PubMed: 30763214]
14. Dinesh NEH, Reinhardt DP. Inflammation in thoracic aortic aneurysms. Herz. 2019;44:138–146. doi: 10.1007/s00059-019-4786-7 [PubMed: 30747234]
15. Pisano C, Balistreri CR, Ricasoli A, Ruvolo G. Cardiovascular Disease in Ageing: An Overview on Thoracic Aortic Aneurysm as an Emerging Inflammatory Disease. Mediators of Inflammation. 2017;2017:1–8. doi: 10.1155/2017/1274034
16. Robinson MD, McCarthy DJ, Smyth GK. edgeR: a Bioconductor package for differential expression analysis of digital gene expression data. Bioinformatics (Oxford, England). 2010;26:139–140. doi: 10.1093/bioinformatics/btp616
17. Maza E. In Papyro Comparison of TMM (edgeR), RLE (DESeq2), and MRN Normalization Methods for a Simple Two-Conditions-Without-Replicates RNA-Seq Experimental Design. Front Genet. 2016;7:164. doi: 10.3389/fgene.2016.00164 [PubMed: 27695478]
18. Reimand J, Kull M, Peterson H, Hansen J, Vilo J. g:Profiler—a web-based toolset for functional profiling of gene lists from large-scale experiments. Nucleic Acids Research. 2007;35:W193–W200. doi: 10.1093/nar/gkm226 [PubMed: 17478515]
19. Szklarczyk D, Gable AL, Nastou KC, Lyon D, Kirsch R, Pyysalo S, Doncheva NT, Legeay M, Fang T, Bork P, et al. The STRING database in 2021: customizable protein–protein networks, and functional characterization of user-uploaded gene/measurement sets. Nucleic Acids Research. 2020;49:D605–D612. doi: 10.1093/nar/gkaa1074
20. Wu S-C, Rau C-S, Kuo P-J, Shih F-Y, Lin H-P, Wu Y-C, Hsieh T-M, Liu H-T, Hsieh C-H. Profiling the Expression of Circulating Acute-Phase Proteins, Cytokines, and Checkpoint Proteins in Patients with Severe Trauma: A Pilot Study. Journal of Inflammation Research. 2021;Volume 14:3739–3753. doi: 10.2147/jir.s324056 [PubMed: 34393495]
21. Zhang X, Xiao Z, Liu X, Du L, Wang L, Wang S, Zheng N, Zheng G, Li W, Dong Z, et al. The potential role of ORM2 in the development of colorectal cancer. PLoS One. 2012;7:e31868. doi: 10.1371/journal.pone.0031868 [PubMed: 22363757]
22. Ye X, Zhang N, Jin Y, Xu B, Guo C, Wang X, Su Y, Yang Q, Song J, Yu W, et al. Dramatically changed immune-related molecules as early diagnostic biomarkers of non-small cell lung cancer. FEBS J. 2020;287:783–799. doi: 10.1111/febs.15051 [PubMed: 31482685]
23. Yu B, Zhu H-D, Shi X-L, Chen P-P, Sun X-M, Xia G-Y, Fang M, Zhong Y-X, Tang X-L, Zhang T, et al. iTRAQ-based quantitative proteomic analysis of thoracic aortas from adult rats born to preeclamptic dams. Clinical Proteomics. 2021;18. doi: 10.1186/s12014-021-09327-9
24. Lourenço AB, Artal-Sanz M. The Mitochondrial Prohibitin (PHB) Complex in C. elegans Metabolism and Ageing Regulation. Metabolites. 2021;11:636. doi: 10.3390/metabo11090636 [PubMed: 34564452]
25. Yan C, Gong L, Chen L, Xu M, Abou-Hamdan H, Tang M, Desaubry L, Song Z. PHB2 (prohibitin 2) promotes PINK1-PRKN/Parkin-dependent mitophagy by the PARL-PGAM5-PINK1 axis. Autophagy. 2020;16:419–434. doi: 10.1080/15548627.2019.1628520 [PubMed: 31177901]

26. Wang W, Qin Y, Song H, Wang L, Jia M, Zhao C, Gong M, Zhao W. Galectin-9 Targets NLRP3 for Autophagic Degradation to Limit Inflammation. The Journal of Immunology. 2021;206:2692–2699. doi: 10.4049/jimmunol.2001404 [PubMed: 33963043]
27. Tyrrell DJ, Blin MG, Song J, Wood SC, Goldstein DR. Aging Impairs Mitochondrial Function and Mitophagy and Elevates Interleukin 6 Within the Cerebral Vasculature. Journal of the American Heart Association. 2020;9. doi: 10.1161/jaha.120.017820
28. Maekawa H, Inoue T, Ouchi H, Jao T-M, Inoue R, Nishi H, Fujii R, Ishidate F, Tanaka T, Tanaka Y, et al. Mitochondrial Damage Causes Inflammation via cGAS-STING Signaling in Acute Kidney Injury. Cell reports. 2019;29:1261–1273.e1266. doi: 10.1016/j.celrep.2019.09.050 [PubMed: 31665638]
29. Pandey S, Kawai T, Akira S. Microbial sensing by Toll-like receptors and intracellular nucleic acid sensors. Cold Spring Harb Perspect Biol. 2015;7:a016246. doi: 10.1101/cshperspect.a016246
30. Takemoto Y, Ramirez RJ, Yokokawa M, Kaur K, Ponce-Balbuena D, Sinno MC, Willis BC, Ghanbari H, Ennis SR, Guerrero-Serna G, et al. Galectin-3 Regulates Atrial Fibrillation Remodeling and Predicts Catheter Ablation Outcomes. JACC Basic Transl Sci. 2016;1:143–154. doi: 10.1016/j.jacbts.2016.03.003 [PubMed: 27525318]
31. Kuang F, Liu J, Xie Y, Tang D, Kang R. MGST1 is a redox-sensitive repressor of ferroptosis in pancreatic cancer cells. Cell Chem Biol. 2021;28:765–775.e765. doi: 10.1016/j.chembiol.2021.01.006 [PubMed: 33539732]
32. Poirier K, Lebrun N, Broix L, Tian G, Saillour Y, Boscheron C, Parrini E, Valence S, Pierre BS, Oger M, et al. Mutations in TUBG1, DYNC1H1, KIF5C and KIF2A cause malformations of cortical development and microcephaly. Nat Genet. 2013;45:639–647. doi: 10.1038/ng.2613 [PubMed: 23603762]
33. Malek N, Michrowska A, Mazurkiewicz E, Mrówczyńska E, Mackiewicz P, Mazur AJ. The origin of the expressed retrotransposed gene ACTBL2 and its influence on human melanoma cells' motility and focal adhesion formation. Sci Rep. 2021;11:3329. doi: 10.1038/s41598-021-82074-x [PubMed: 33558623]
34. Org E, Eyheramendy S, Juhanson P, Gieger C, Lichtner P, Klopp N, Veldre G, Döring A, Viigimaa M, Sõber S, et al. Genome-wide scan identifies CDH13 as a novel susceptibility locus contributing to blood pressure determination in two European populations. Hum Mol Genet. 2009;18:2288–2296. doi: 10.1093/hmg/ddp135 [PubMed: 19304780]
35. Sharma UC, Pokharel S, van Brakel TJ, van Berlo JH, Cleutjens JP, Schroen B, André S, Crijns HJ, Gabius HJ, Maessen J, et al. Galectin-3 marks activated macrophages in failure-prone hypertrophied hearts and contributes to cardiac dysfunction. Circulation. 2004;110:3121–3128. doi: 10.1161/01.CIR.0000147181.65298.4D [PubMed: 15520318]
36. Hua X, Hu G, Hu Q, Chang Y, Hu Y, Gao L, Chen X, Yang PC, Zhang Y, Li M, et al. Single-Cell RNA Sequencing to Dissect the Immunological Network of Autoimmune Myocarditis. Circulation. 2020;142:384–400. doi: 10.1161/CIRCULATIONAHA.119.043545 [PubMed: 32431172]
37. Pober JS, Merola J, Liu R, Manes TD. Antigen Presentation by Vascular Cells. Frontiers in immunology. 2017;8:1907–1907. doi: 10.3389/fimmu.2017.01907 [PubMed: 29312357]
38. Li Y, Lemaire SA, Shen YH. Molecular and Cellular Dynamics of Aortic Aneurysms Revealed by Single-Cell Transcriptomics. Arteriosclerosis, Thrombosis, and Vascular Biology. 2021. doi: 10.1161/atvbaha.121.315852
39. Luo W, Wang Y, Zhang L, Ren P, Zhang C, Li Y, Azares AR, Zhang M, Guo J, Ghaghada KB, et al. Critical Role of Cytosolic DNA and Its Sensing Adaptor STING in Aortic Degeneration, Dissection, and Rupture. Circulation. 2020;141:42–66. doi: doi:10.1161/CIRCULATIONAHA.119.041460 [PubMed: 31887080]
40. Miura Y, Tsumoto H, Iwamoto M, Yamaguchi Y, Ko P, Soejima Y, Yoshida S, Toda T, Arai T, Hamamatsu A, et al. Age-associated proteomic alterations in human aortic media. Geriatr Gerontol Int. 2019;19:1054–1062. doi: 10.1111/ggi.13757 [PubMed: 31436032]
41. Sanese P, Forte G, Disciglio V, Grossi V, Simone C. FOXO3 on the Road to Longevity: Lessons From SNPs and Chromatin Hubs. Comput Struct Biotechnol J. 2019;17:737–745. doi: 10.1016/j.csbj.2019.06.011 [PubMed: 31303978]

42. Tan KL, Haelterman NA, Kwartler CS, Regalado ES, Lee PT, Nagarkar-Jaiswal S, Guo DC, Duraine L, Wangler MF, Bamshad MJ, et al. Ari-1 Regulates Myonuclear Organization Together with Parkin and Is Associated with Aortic Aneurysms. Dev Cell. 2018;45:226–244.e228. doi: 10.1016/j.devcel.2018.03.020 [PubMed: 29689197]
43. Zamorano-Leon JJ, Serna-Soto M, Moñux G, Freixer G, Zekri-Nechar K, Cabrero-Fernandez M, Segura A, Gonzalez-Cantalapiedra A, Serrano J, Farré AL. Factor Xa Inhibition by Rivaroxaban Modified Mitochondrial-Associated Proteins in Human Abdominal Aortic Aneurysms. Ann Vasc Surg. 2020;67:482–489. doi: 10.1016/j.avsg.2020.02.005 [PubMed: 32173474]
44. Gaidt MM, Ebert TS, Chauhan D, Ramshorn K, Pinci F, Zuber S, O'Duill F, Schmid-Burgk JL, Hoss F, Buhmann R, et al. The DNA Inflammasome in Human Myeloid Cells Is Initiated by a STING-Cell Death Program Upstream of NLRP3. Cell. 2017;171:1110–1124.e1118. doi: 10.1016/j.cell.2017.09.039 [PubMed: 29033128]
45. Bai J, Liu F. The cGAS-cGAMP-STING Pathway: A Molecular Link Between Immunity and Metabolism. Diabetes. 2019;68:1099–1108. doi: 10.2337/dbi18-0052 [PubMed: 31109939]
46. Wang S, Zhang X, Yuan Y, Tan M, Zhang L, Xue X, Yan Y, Han L, Xu Z. BRG1 expression is increased in thoracic aortic aneurysms and regulates proliferation and apoptosis of vascular smooth muscle cells through the long non-coding RNA HIF1A-AS1 in vitro. European Journal of Cardio-Thoracic Surgery. 2015;47:439–446. doi: 10.1093/ejcts/ezu215 [PubMed: 24875884]
47. He R, Guo D-C, Estrera AL, Safi HJ, Huynh TT, Yin Z, Cao S-N, Lin J, Kurian T, Buja LM, et al. Characterization of the inflammatory and apoptotic cells in the aortas of patients with ascending thoracic aortic aneurysms and dissections. The Journal of Thoracic and Cardiovascular Surgery. 2006;131:671–678.e672. doi: 10.1016/j.jtcvs.2005.09.018 [PubMed: 16515922]
48. Minderhoud SCS, Roos-Hesselink JW, Chelu RG, Bons LR, Van Den Hoven AT, Korteland S-A, Van Den Bosch AE, Budde RPJ, Wentzel JJ, Hirsch A. Wall shear stress angle is associated with aortic growth in bicuspid aortic valve patients. European Heart Journal - Cardiovascular Imaging. 2022. doi: 10.1093/ehjci/jeab290
49. Wilkins HM, Weidling IW, Ji Y, Swerdlow RH. Mitochondria-Derived Damage-Associated Molecular Patterns in Neurodegeneration. Frontiers in immunology. 2017;8:508–508. doi: 10.3389/fimmu.2017.00508 [PubMed: 28491064]

Highlights:

- Human aging transforms the aortic proteome in health and in thoracic aortic aneurysm.
- In the young cohort, immunological processes are enriched within the human aorta from health to thoracic aortic aneurysm.
- In the old cohort, metabolic processes are enriched within the human aorta from health to thoracic aortic aneurysm.

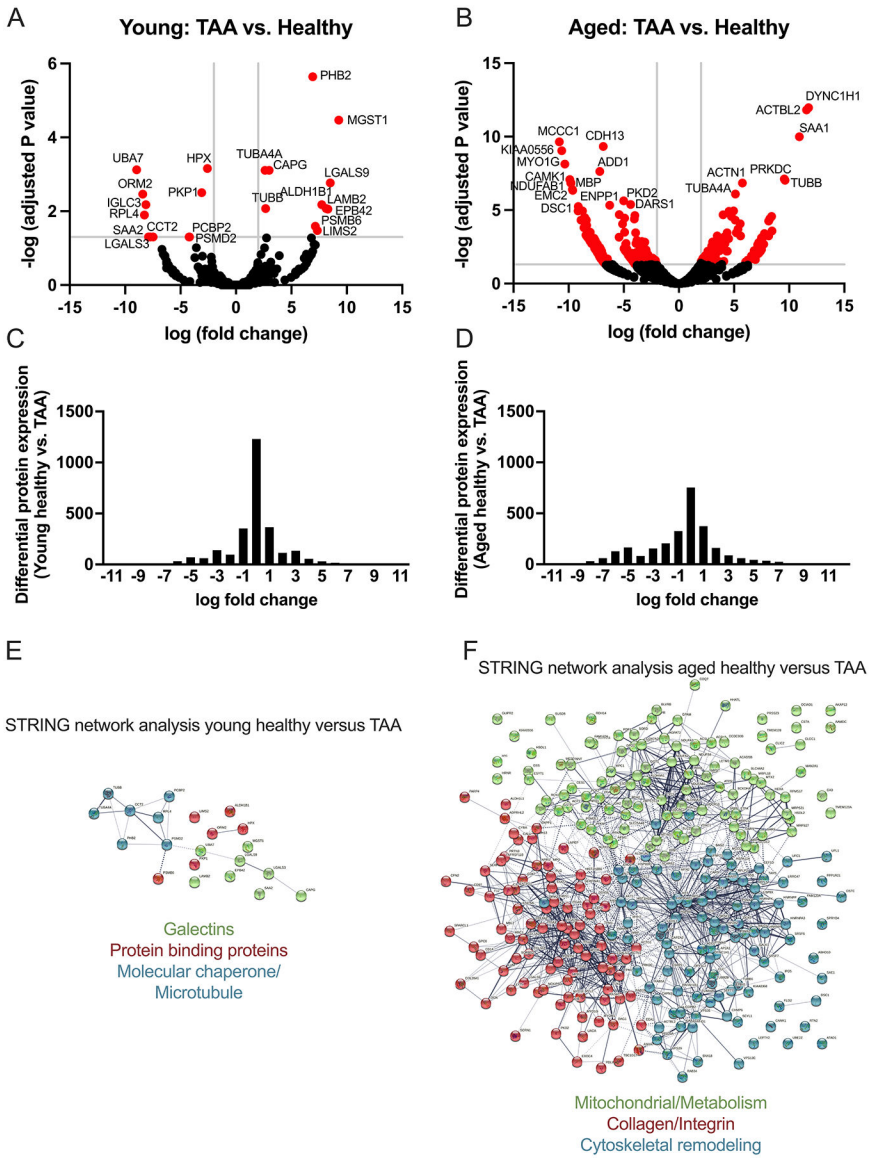

Figure 1: Aging transforms the aortic proteome comparing health to TAA.

Aortic samples from healthy subjects and those that underwent repair for TAA were assessed via mass spectrometry. Specimens were categorized into young (i.e., <60 years of age) and aged (i.e., ≥60 years of age) in both the healthy and TAA group. N = 4 biological specimens for each group. All TAA specimens had bicuspid aortic values. Raw spectral counts were adjusted for false discovery rate and the healthy were compared to the TAA in each of the age groups, and displayed in volcano plots for young (**A**) and aged (**B**). Proteins with $-\log_{10}$ (adjusted P value) >3 and $\log_{10}$ (fold change) <2 and >2 are colored red and the 20 proteins with most significant adjusted P value are labeled with protein name. **C and D:** Histograms of the log fold-change of all differentially expressed proteins comparing healthy vs. TAA for young (**C**) and aged (**D**). **E and F**: Using STRING database search, we performed network analysis to identify the top 3 most interconnected networks and identified the common processes within each network for young healthy vs. TAA (**E**) and aged healthy vs. TAA (**F**).

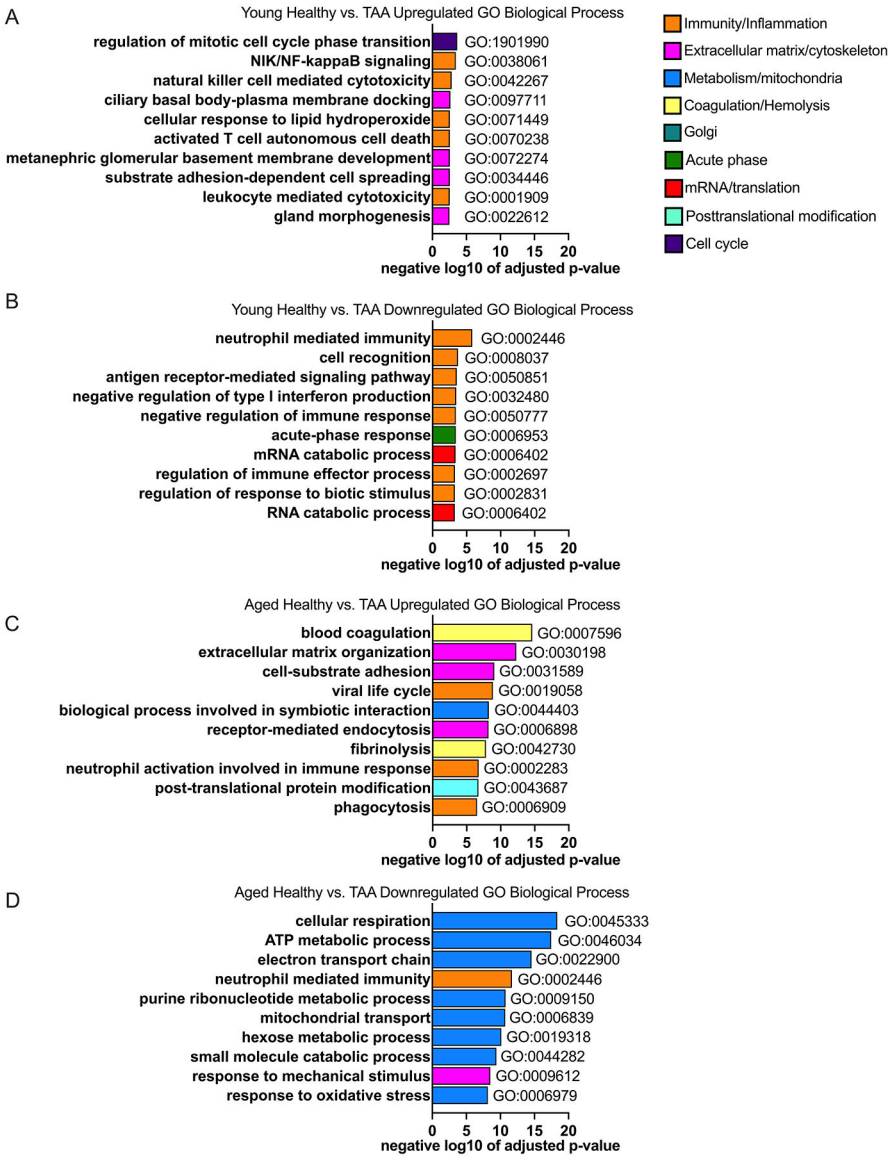

Figure 2: Biologically different processes and networks are impacted by TAA in young as compared to older cohort

Aortic samples were assessed via mass spectrometry. Young (i.e., <60 years of age) and old (i.e., >60 years of age) in the healthy and TAA groups were compared. N = 4 biological specimens for each group. **A and B:** Top 10 gene ontology (GO) biological processes from proteins that were significantly up- (**A**) and down- (**B**) regulated comparing healthy aortic samples to samples from TAA in the young group and sorted by adjusted p-value. **C and D:** Top 10 gene ontology (GO) biological processes from proteins that were significantly up- (**C**) and down- (**D**) regulated comparing healthy aortic samples to samples from TAA in the aged group and sorted by adjusted p-value. GO biological processes within similar categories were color coded the same. Blue encodes metabolic and mitochondrial processes, orange encodes immune and inflammatory processes, yellow encodes hemolysis and coagulation processes, pink encodes cytoskeletal and extracellular matrix processes, cyan encodes posttranslational modifications, teal encodes golgi-related processes, green

encodes acute phase proteins, red encodes mRNA processes, and purple encodes cell cycle processes.

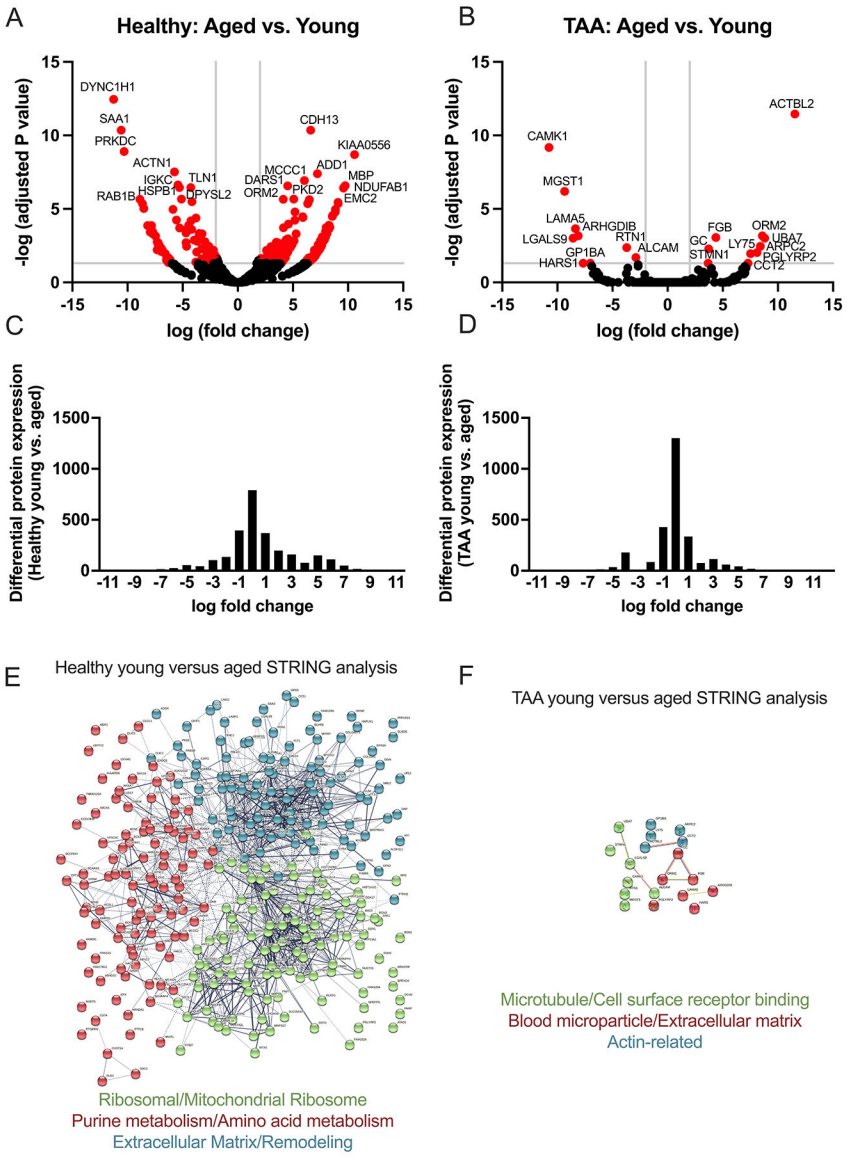

Figure 3: Aging dysregulates more proteins and processes in the aorta in health compared with TAA.

Aortic samples were assessed via mass spectrometry. Young (i.e., <60 years of age) and aged (i.e., >60 years of age) in the healthy, and also in the TAA groups were compared. N = 4 biological specimens / group. Raw spectral counts were adjusted for false discovery rate and displayed in volcano plots for healthy (**A**) and TAA (**B**). Proteins with −log (adjusted P value) >3 and log (fold change) <2 and >2 are colored red and the 20 proteins with most significant adjusted P value are labeled with protein name. **C and D:** Histograms of the log fold-change of all differentially expressed proteins comparing young vs. aged for healthy (**C**) and TAA (**D**). **E and F**: Using STRING database search, we performed network analysis to identify the top 3 most interconnected networks and identified the common processes within each network for healthy young vs. age (**E**) and TAA young vs. aged (**F**). A=aged, Y=young.

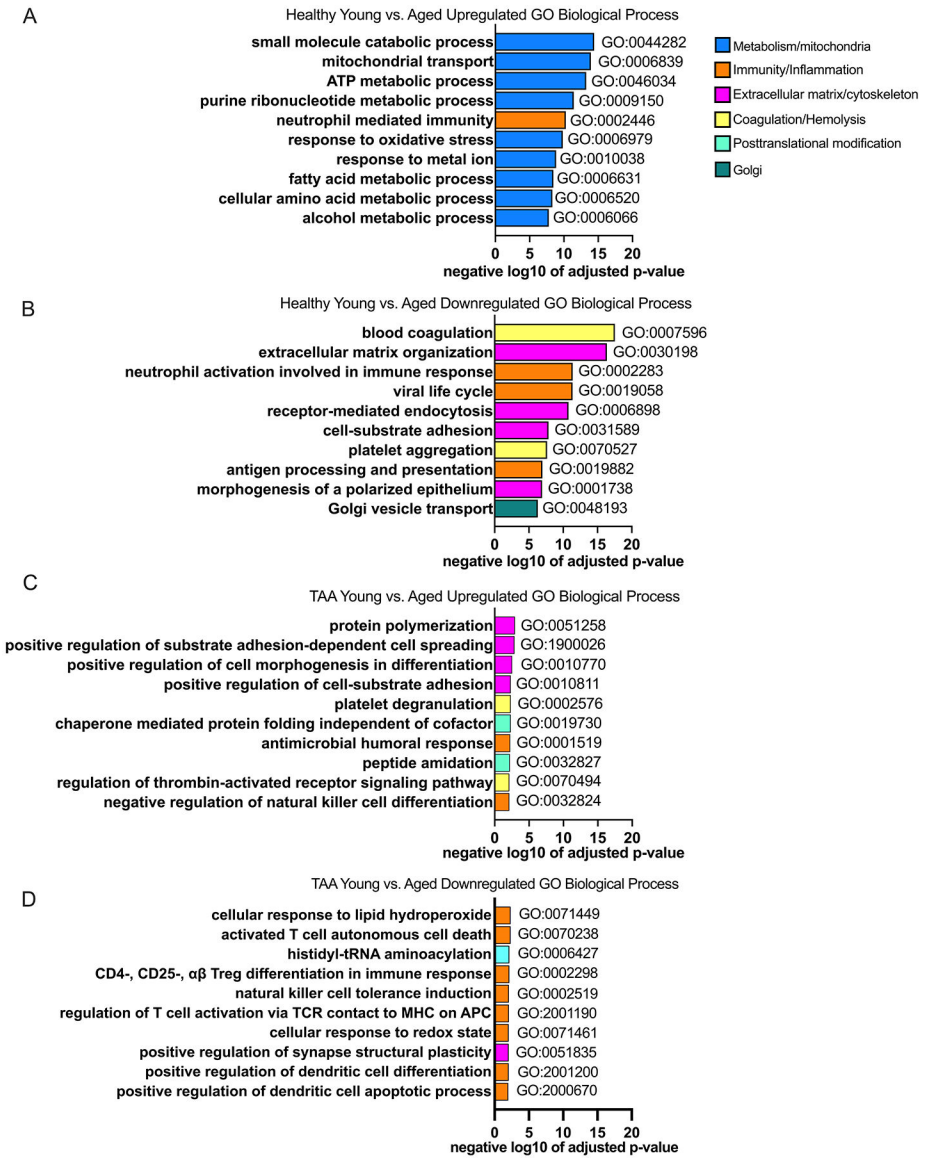

Figure 4: Aging dysregulates more processes in the aorta in health compared to TAA

Aortic samples were assessed via mass spectrometry. Young (i.e., <60 years of age) and old (i.e., >60 years of age) in the healthy and TAA groups were compared. N = 4 biological specimens / group. **A and B:** Top 10 gene ontology (GO) biological processes from proteins that were significantly up- (**A**) and down- (**B**) regulated in the healthy group comparing aged to young and sorted by adjusted p-value. **C and D:** Top 10 GO biological processes from proteins that were significantly up- (**C**) and down- (**D**) regulated in the TAA group comparing aged to young and sorted by adjusted p-value. GO biological processes within similar categories were color coded the same. Blue encodes metabolic and mitochondrial processes, orange encodes immune and inflammatory processes, yellow encodes hemolysis and coagulation processes, pink encodes cytoskeletal and extracellular matrix processes, cyan encodes posttranslational modifications, and teal encodes golgi-related processes.

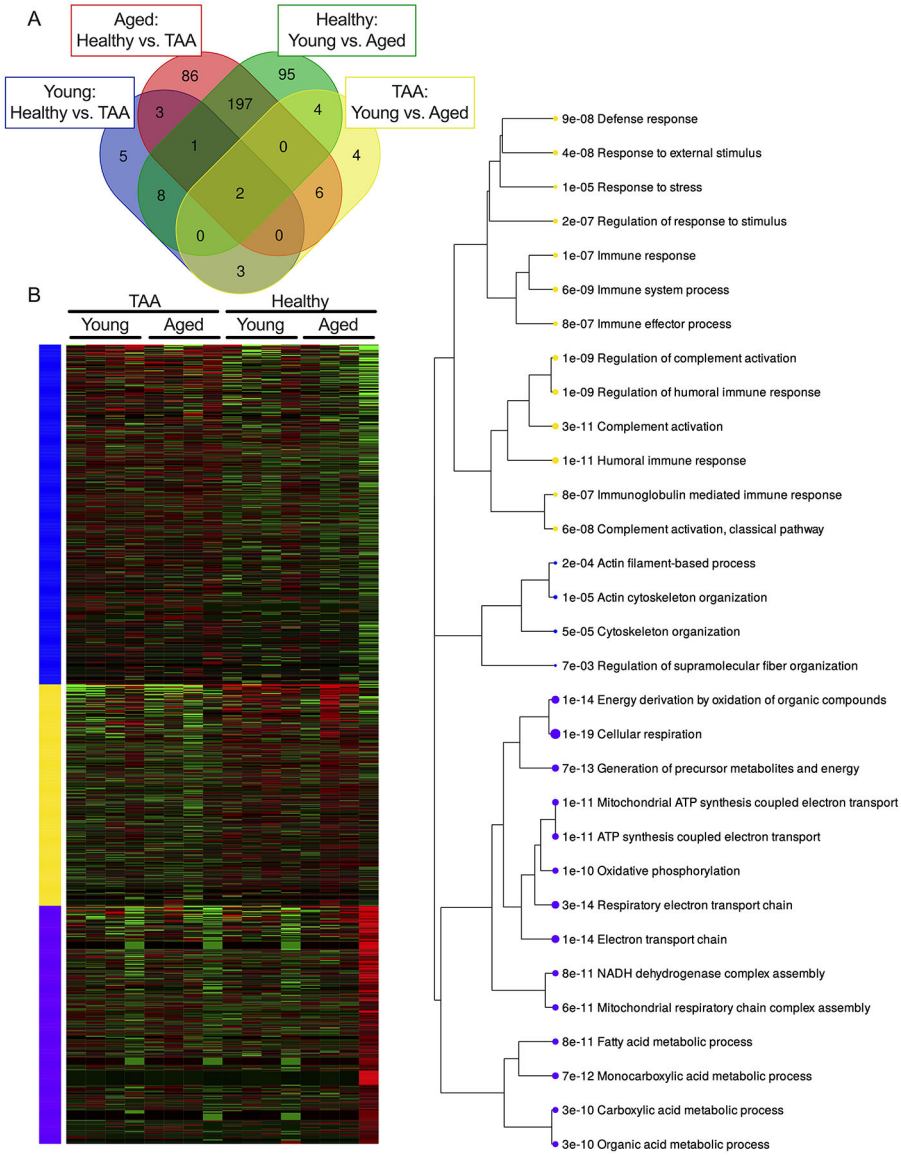

Figure 5. Aging and TAA significantly alter the proteome with some overlapping differentially expressed proteins.

Aortic samples from Young (i.e., <60 years of age) and aged (i.e., >60 years of age) subjects in both the healthy and TAA groups were assessed via mass spectrometry with N = 4 biological specimens / group (total of 16 samples). Raw spectral counts were adjusted for false discovery rate and log2 normalized. Proteins that met the false discovery rate adjusted P-value (0.05) were considered statistically significant. **A**: Venn diagram showing the number of shared differentially expressed proteins between the 4 comparisons (Young Healthy vs. TAA, Aged Healthy vs. TAA, Healthy Young vs. Aged, and TAA Young vs. Aged) that were analyzed. **B**: Unsupervised K-means clustering heatmap of the differentially expressed proteins identified. **C**: Enrichment plot of shared gene ontology biological processes identified by K-means clustering in **B** where the size of the dot indicates the number of proteins identified for each GO biological process and the number represents

adjusted p-value of the biological process. Blue, yellow, and purple colors signify groups of related proteins identified by K-means clustering in **B** and described in **C**.

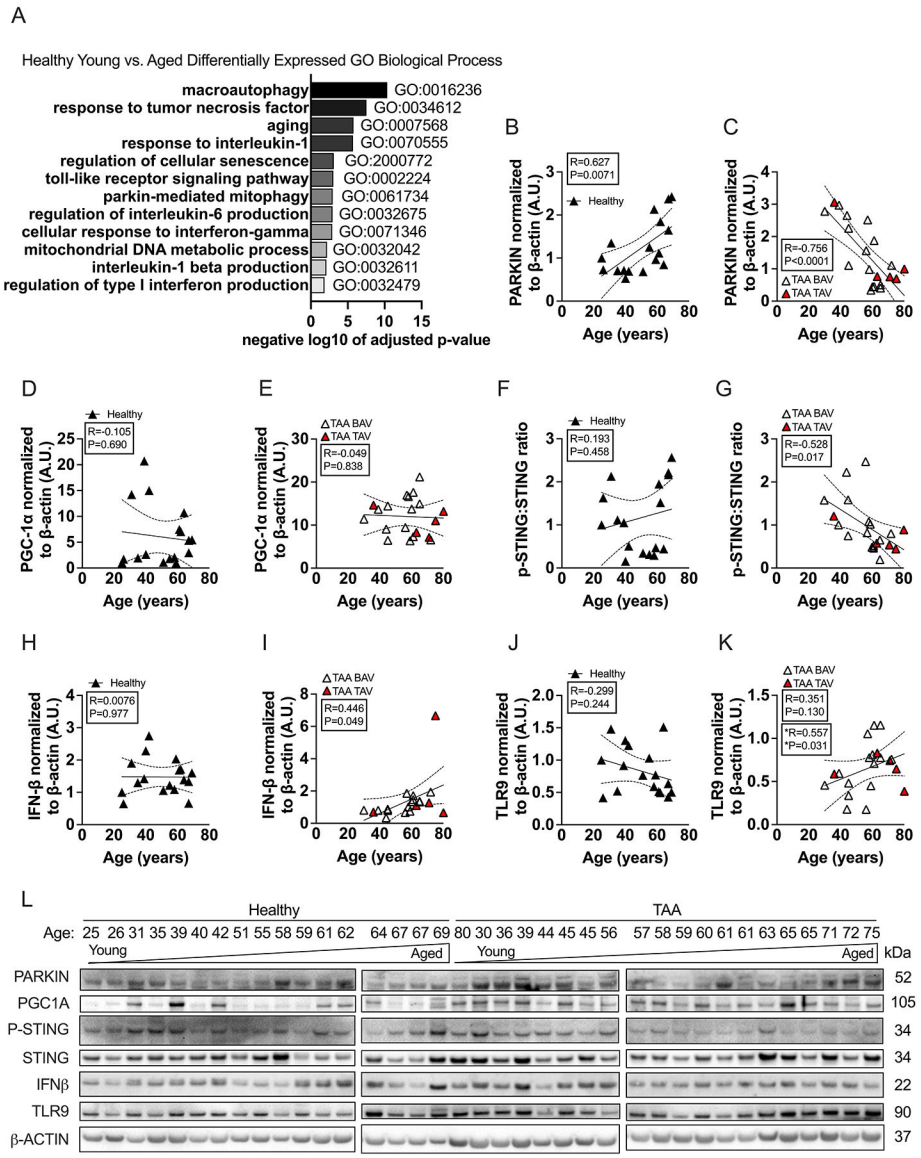

Figure 6. TAA modifies how aging impacts Parkin and the pSTING:STING, TLR9, IFN-β axis in the aorta compared to health.

Aortic samples from healthy subjects were assessed via mass spectrometry. Young (i.e., <60 years of age) and old (i.e., >60 years of age) in the healthy group were compared. N = 4 biological specimens for each group. **A**: Targeted search of statistically significant gene ontology (GO) biological processes from proteins that were significantly up- and down-regulated by adjusted p-value were identified. GO terms that were searched for were: “autophagy”, “tumor necrosis factor”, “aging”, “interleukin”, “senescence”, “toll-like receptor”, “parkin”, “mitophagy”, “interferon”, and “mitochondria”; which were ordered based on statistical significance level. **B**-**L**: Aortic lysates from healthy (N = 17) and TAA (N = 20) subjects were immunoblotted against PARKIN, PPARγ co-activator 1 α (PGC1α), stimulator of interferon genes (STING), phosphorylated-STING (p-STING), interferon-β (IFN-β), toll-like receptor 9 (TLR9), and β-actin. PARKIN (**B**-**C**), PGC1α (**D**-**E**), the ratio of p-STING to STING (**F**-**G**), IFN-β (**H**-**I**), and TLR9 (**J**-**K**) expression in the healthy

and TAA groups, were plotted against age and regression analysis was performed. **L:** All immunoblots for PARKIN, PGC1α, p-STING to STING, IFN-β, TLR9, and β-actin along with subject age are shown. Note, that the 80-yr old TAA sample was erroneously place out of order. BAV = bicuspid aortic valve (open triangle), TAV = triscupid aortic valve (red triangle). P values and correlation coefficients represent all data points within each graph. *P values and correlation coefficient represents only the BAV data in **K**.

Table 1:

Subject Demographics

	Healthy Young	Healthy Aged	TAA Young	TAA Aged
N	11	6	10	10
Age, mean (SD)	41.9 (12.3)	65.0 (3.2) *	46.9 (10.2) $	67.3 (6.8) **,‡
Female, n (%)	3 (27.3)	1 (16.7) †	5 (50.0) $	5 (50.0) ‡, #
Aneurysm diameter, mm (SD)	N/A	N/A	44.3 (10.1)	48.4 (6.2) #
Comorbidities				
BAV, n (%)	N/A	N/A	10 (100)	9 (90) #
CKD n, (%)	N/A	N/A	9 (90)	6 (60) #
ICM, n (%)	N/A	N/A	1 (10)	1 (10) #
NICM, n (%)	N/A	N/A	0 (0)	0 (0) #
Atrial Fibrillation, n (%)	N/A	N/A	0 (0)	0 (0) #
LV Assist Device, n (%)	N/A	N/A	3 (30)	4 (40) #
Hyperlipidemia, n (%)	N/A	N/A	0 (0)	0 (0) #
Type 2 Diabetes, n (%)	N/A	N/A	1 (10)	2 (20) #
Hypertension, n (%)	N/A	N/A	0 (0)	1 (10) #
Atherosclerosis, n (%)	N/A	N/A	7 (70)	6 (60) #

Demographics of subjects in this study. BAV=bicuspid aortic valve, CKD=chronic kidney disease, ICM=ischemic cardiomyopathy, NICM=non-ischemic cardiomyopathy, TAA=thoracic aortic aneurysm.

* P<0.001 healthy aged vs. healthy young

** P<0.0001 TAA aged vs. TAA young

† = not significant healthy aged vs. healthy young

$ = not significant TAA young vs. healthy young.

‡ = not significant TAA aged vs. healthy aged

= not significant TAA aged vs. TAA young. All comparisons between comorbidities are non-significant. Significance for sex and comorbidities determined by Fisher's Exact test. Significance for age and aneurysm diameter determined by Mann-Whitney U test.